Resonance measurements of d-f-g-h intervals in Rydberg states of sodium and a redetermination of the core polarizabilities

L. G. Gray, X. Sun, and K. B. MacAdam
Department of Physics and Astronomy, University of Kentucky, Lexington, Kentucky 40506-0055
(Received 11 April 1988)

Microwave resonances in Na Rydberg states $n=22-30$ between d, f, g, and h states have been detected by field ionization. The 39 new transition frequencies have been combined with previously measured frequencies in the same Rydberg series, $n=9-17$, in order to test the internal consistency and reliability of the data by using series formulas. A new analysis of the effective dipole and quadrupole core polarizabilities in Na^+, based on the enlarged data set, has been carried out, and the sensitivity of the results to several model assumptions has been examined. The results are $\alpha_d'=0.9980\pm0.0033$ a.u. and $\alpha_Q'=0.351\pm0.081$ a.u.

I. INTRODUCTION

In our studies of l change induced by ion impact on Na(nd) atoms in Rydberg states[1,2] we have recently found a significant broadening in the distribution of final l states as the projectile velocity $v_{\rm ion}$ is reduced below the matching velocity, i.e., for $\tilde{v}<1$.[3,4] (The reduced velocity $\tilde{v}$ equals $v_{\rm ion}/v_{\rm Bohr}$, where $v_{\rm Bohr}$ is the Bohr-orbital velocity of state n.) In order to quantify the variation of final-state distributions we have measured selective field ionization (SFI) signals following exposure of a state-selected Na 28d Rydberg target to ion impact and have fitted them by a superposition of SFI signals corresponding to resolved l values, $l\geq3$. Single-collision conditions were maintained. The resolved-l signals, obtained in preliminary work by numerical simulation of the field ionization of corresponding hydrogen Stark sublevels,[3] have more recently been recorded experimentally by using microwave-resonance techniques to drive transitions from 28d to 28f, g, and h states.[4] Further development of this technique for the study of l-change collisions must rest on accurate spectroscopy of Na $l\geq3$ states in the range of principal quantum numbers used for collisions. The required accuracy (≤1 MHz) is set ultimately by the natural (radiative) widths of the levels but in practice is set by broadening due to irreducible stray fields. Furthermore, since electric fields as small as 10 mV/cm can cause Stark mixing and the loss of pure angular momentum character the careful study of microwave resonances offers a sensitive probe of ambient fields that may significantly affect collisional outcomes.[5]

We have carried out extensive measurements of Na nd-nf, nd-ng, and nd-nh transitions by single- and multiphoton resonance at frequencies 3–9 GHz for $n=22-30$, obtaining line widths narrower than 1 MHz in favorable cases. We report 39 new level separations with resolved fine structure. Gallagher *et al.* have previously measured the corresponding transitions for $n=13-17$,[6,7] but extrapolation of their results to $n\geq22$ was not sufficiently reliable for the present purpose.

Freeman and Kleppner[8] determined Na core electric dipole and quadrupole polarizabilities from the experimental microwave-resonance data of Gallagher *et al.*[6,7] In their analysis using this relatively restricted data set, Freeman and Kleppner assumed that the spin-orbit fine structure of f, g, and h states was hydrogenic. They included the effect of core penetration by using first-order perturbation theory and Na^+ wave functions to calculate the penetration energies for f states. (Penetration was negligible for g and h states.) The polarization shifts themselves were modeled by perturbation theory[9] using hydrogenic expectation values $\langle r^{-4}\rangle$ and $\langle r^{-6}\rangle$. More recently this analysis has been reexamined by several authors, without, however, any addition to the Rydberg data set. Specifically, see the following.

(1) Theodosiou[10] has calculated penetration energies in first-order perturbation theory using a variety of core wave functions, comparing in particular the results from ground-state wave functions of the Na^+ ion with those from the Na^+ core of neutral ground-state Na. The results showed a 13% range of values for nf penetration, well within the 33% error bars set by Freeman and Kleppner and with values considerably smaller than for open-shell cores, but opening to question the appropriate manner of making penetration corrections in an evaluation of core polarizabilities.

(2) Lombardi[11] investigated whether perturbation theory itself was sufficiently accurate by comparing several perturbative results for penetration and polarization with a direct numerical integration of the Schrödinger equation for Na, $n=13-17$ f and g states. Numerical integration yielded f-state penetration energies larger by about 21% than those of Freeman and Kleppner.

(3) Patil[12] recently pointed out that in the analysis of Na Rydberg levels, direct penetration must be combined with exchange penetration and with certain distortion corrections that appear along with polarization in the second-order Born term. Penetration, exchange, and distortion for Na f states in the limit $n\rightarrow\infty$ stand in the approximate ratios 1:2:−1, and thus their sum equals twice the penetration effect that was previously allowed for.

(4) In microwave experiments subsequent to those establishing the original d-f-g-h data set, Gallagher and

co-workers[13,14] determined that the Na Rydberg f-state spin-orbit fine-structure splitting is about 5% smaller than hydrogenic.

In the light of all these developments, a reanalysis of the Na core polarizability is required. In Sec. II the experimental method will be described, and in Sec. III the new spectroscopic measurements will be presented. Section IV reviews the prior data. In Sec. V we discuss series fitting formulas for Rydberg level separations, correct the present measurements for small Stark shifts, and demonstrate that the previously available data apparently contained experimental errors considerably in excess of original estimates. A reanalysis of Na core polarizabilities is presented and discussed in Sec. VI, and conclusions are drawn in Sec. VII.

II. EXPERIMENTAL METHOD

Most aspects of the apparatus and techniques have been described in previous publications.[1,2,4] (In the description below, the z axis is vertically upward from an origin at the center of the Rydberg-atom region.) A sodium thermal atomic beam of density about 10^8 cm^{-3} passes in the $+y$ direction into an interaction region where about 1% of the atoms in a few-mm^3 volume are excited stepwise to the $22d-30d$ states by pulsed laser beams polarized in the xy plane (Fig. 1). The first excitation occurs to the $3p_{3/2}$ (or $3p_{1/2}$) level in a "yellow" beam at 589.0 nm (or 589.6 nm) that enters the interaction region in the $-z$ direction. The second excitation is provided by a 410-nm "blue" beam that enters in the $-y$ direction. Excitation through the $3p_{3/2}$ state populates both $nd_{3/2}$ and $nd_{5/2}$ fine-structure levels, but excitation through $3p_{1/2}$ populates only $nd_{3/2}$. Both excitation schemes are used in this work in order to clarify the identification of the microwave resonances.

The Rydberg atoms lie between horizontal condensor plates that are separated by 1.3 cm. A few μs after each laser flash a high-voltage pulse or ramp is applied to the upper plate for selective field ionization. The lower plate is biased by a variable low voltage, $|V_{\text{bias}}| < 1$ V, which

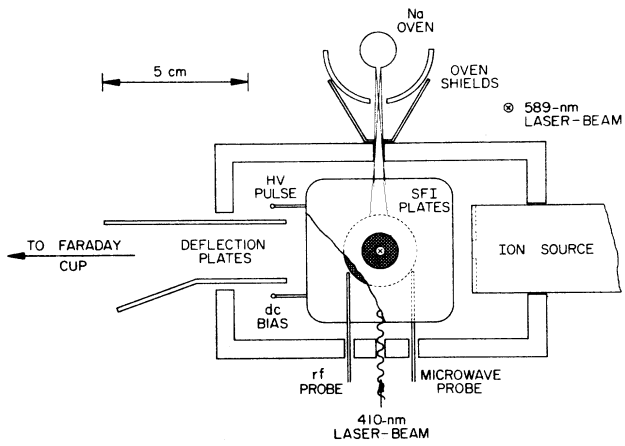

FIG. 1. Interaction region of the apparatus (view from above). The ion source, ion deflection plates, and Faraday cup used for associated collision experiments are also shown.

may be used to null any uniform vertical electric-field background. Na^+ ions produced in the SFI field are accelerated downward through a fine-mesh grid (60 lines/in.) into a discrete-dynode electron multiplier whose anode signal is recorded both by an analog gated integrator and a 100-MHz transient digitizer[15] under computer control. For $n < 32$, $|m_l| = 0$, 1, and 2 sublevels of Na Rydberg states ionize adiabatically near the classical threshold field, $1/16n^4$ a.u.[16] However, $|m_l| \geq 3$ sublevels ionize diabatically at fields roughly twice as large.[17] Transfer from $|m_l| = 2$ to higher $|m_l|$ levels is thus readily detectable by SFI. (This fact has formed the basis for our previous measurements of l change under ion bombardment.[1,2,4]) Two horizontal wire probes of 1.6 mm diameter are inserted between the condensor plates in their median plane and parallel to the y axis so that the rounded probe tips each lie 1.3 cm horizontally from the center of the volume of Rydberg atoms.[18] The first probe is connected to a Hewlett-Packard (HP) 8673E synthesized microwave oscillator (2–18 GHz), and the second probe is connected to an HP 8656A synthesized rf oscillator (0.1–990 MHz). The probes introduce weak horizontal (nonuniform) oscillating electric fields in the region of the Rydberg atoms that drive transitions from the $|m_l| = 2$ sublevels to higher $|m_l|$ sublevels by electric-dipole transitions. (Transitions populating $|m_l| \leq 2$ sublevels in the final state are also driven but are not readily detectable using SFI.) Both oscillators are pulsed off prior to the application of any SFI detection pulse. This avoids quantum interference between Stark levels that could occur during the onset of the rising SFI electric field.[18]

The d-f transitions are single-photon electric-dipole transitions that require only the HP 8673E oscillator at 3–9 GHz. Following laser excitation to nd states in the presence of the weak oscillating field, transitions to nf occur during the 3-μs microwave exposure time. The SFI electric field pulse begins 1 μs after the microwaves are turned off. The SFI pulse magnitude or ramp slope is adjusted for each transition so that the diabatic SFI signal corresponding to the final state is well separated from the adiabatic or partially adiabatic signal of the nd state. The signals are accumulated over one or more 256-laser-shot cycles. The gated-integrator output is digitized and serves as a normalization to remove variations in the diabatic signal that are caused by fluctuations in overall Rydberg-atom production. At each oscillator frequency the displayed transient-digitizer record is summed between preset cursors and is normalized to measure the diabatic signal of the final state. The frequency scan is carried out automatically under computer control through an IEEE-488 interface. The d-f transitions are quite strong and require only about 4 μW incident power (ignoring losses in the crude microwave coupling circuit). For multiphoton transitions to the ng and nh state through virtual levels the microwave frequency is applied as before to one of the probes (well off resonance from the nf state) together with rf at 300–950 MHz (power up to 1 W) applied to the second probe. The rf frequency is fixed, to avoid the effects of transmission-line resonances, while the microwaves are scanned through the multipho-

ton resonance. The d-g level separations correspond to the sum of rf and microwave oscillator frequencies $\nu_{rf}+\nu_{mw}$, and the d-h separations correspond to $2\nu_{rf}+\nu_{mw}$. Downward rf Stark shifts as large as several MHz, linear in the power of the lower-frequency generator, are observed and extrapolated to zero. No shifts were observed as a function of applied microwave power up to 20 mW.

Ambient magnetic fields are nulled to less than 30 mG in the xy plane and 120 mG in the z direction. The components in x and y directions are nulled by measuring the rate of Larmor precession of Rydberg sublevels. In the absence of any microwave or rf radiation the $|m_l|$ content (referred to the z axis) of the fine-structure Zeeman state $|j,m_j\rangle$ oscillates as the magnetic dipole moment precesses about a field not aligned in the z direction. As a function of time delay of the SFI pulse relative to the blue laser flash, the SFI signal exhibits a periodic variation between almost exclusively $|m_l|=0$ character and a mixture of $|m_l|=0$, 1, and 2.[19] The precession frequency is measured from the period of this variation and is proportional to the magnitude of the component of magnetic field in the xy plane. Three mutually orthogonal pairs of field-cancelling coils are mounted symmetrically around the Rydberg interaction region. As the current in the x or y coil pair is varied, the precession frequency exhibits a symmetric minimum about the null point of the corresponding component of the ambient magnetic field. In order to null the z field, which does not lead to precession visible in the SFI signals, a series of microwave spectra are taken as a function of current in the z coils. The spectra exhibit Zeeman splittings that are symmetric about the null point.

Na Rydberg atoms in d, f, g, and h states have very large Stark shifts in static fields. In this work Stark shifts are manifested in two ways: (1) by an asymmetric broadening of the resonance line shape toward lower frequencies, and (2) by a downward shift of the resonance peak. The first effect is a signature of inhomogeneous electric fields in the Rydberg region as well as of differential Stark shifts of unresolved resonance components. This effect is minimized by assuring that the plates and grids are flat, parallel, and "cured" by being uniformly coated with Na from the atomic-beam oven. Curing can require several days at normal oven temperatures but can be accelerated at higher temperatures. In addition, the rf probes are dc coupled to the lower plate and biased in common with it. Resonance line shapes exhibiting more than a minimum asymmetry are rejected. In order to estimate the residual electric field in the z direction, the apparent Stark shift was measured as a function of V_{bias} around the optimum line-shape-symmetrizing value for the $28d_{5/2}$-$28f_{7/2}$ transition under typical operating conditions. About the operating point (144 mV for that run) the line center exhibited a quadratic Stark shift -5.6×10^{-4} MHz mV^{-2}. A shift as small as 0.25 MHz would be readily discernible, thus indicating that the net electric field in the z direction could be nulled to better than 20 mV/cm. Residual fields in the xy plane were not under direct experimental control. However, as described below in Sec. V B, it was determined, based on an examination of the n dependence of the resonance frequencies in each series, that an average total residual field 21 ± 12 mV/cm was present during the measurements.

III. NEW RESULTS

New transitions observed in this work are listed in Table I. (The tabulated resonance frequencies have been corrected for Stark shifts.) Typical frequency scans are shown in Fig. 2. Cavity resonances (i.e., geometric effects on the standing-wave pattern in the interaction region) made it impossible to observe some of the multiphoton resonances in the range $n=22-30$. Weak $\Delta j=\Delta l-1$ resonances were detectable in several cases as partially resolved or unresolved components in stronger lines, but their frequencies could not be accurately determined, and they are not needed for the analysis reported below.

Typical full widths at half maximum (FWHM) for the d-f transitions ranged from 1 MHz for the $23d$-$23f$ to 2.3 MHz for the $26d$-$26f$ without power broadening. The d-h transitions are most severely affected by inhomogeneous stray electric fields and by differential rf Stark shifts, and they exhibited FWHM from 3.7 MHz at $n=23$ to 7 MHz at $n=26$. Although these linewidths were much wider than would be expected from radiative decay alone [less than 0.1 MHz (Ref. 20)] the line shapes were very well defined, and their centers could be determined within standard deviations (SD) 0.5 MHz (d-f and d-g) or 1.2 MHz (d-h). Day-to-day reproducibility within these limits was obtained provided that a thorough curing was allowed. Without curing, the spectra were unusable, apparently due to contact potentials and field irre-

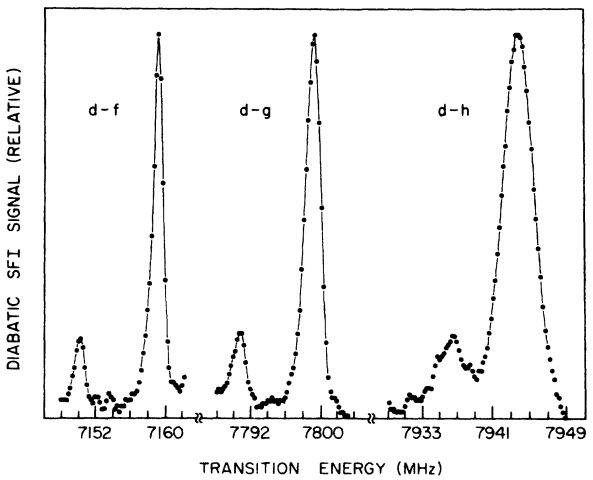

FIG. 2. Microwave resonance scans of the $23d$-$23l$ transitions: (a) $23d$-$23f$ (single photon); (b) $23d$-$23g$ (two photon) with rf oscillator at 950 MHz and microwaves scanned near 6845 MHz; (c) $23d$-$23h$ (three photon) with rf oscillator at 547 MHz and microwaves scanned near 6845 MHz. In each case the lower-frequency peak is $23d_{3/2}$-$23l_{l-1/2}$, and the higher-frequency peak is $23d_{5/2}$-$23l_{l+1/2}$. A very small component $23d_{5/2}$-$23l_{l-1/2}$ is unresolved from the larger peak. The $23d$ state was excited through the $3p_{3/2}$ intermediate state.

TABLE I. Level separations (MHz) based on new microwave resonance measurements in Rydberg states of Na and corrected for residual Stark shifts. The entries for missing measurements indicated by square brackets were calculated from the higher-j components by using fitted d-state fine structure (Table II) and assuming hydrogenic fine structure for g and h states. 1-SD uncertainties, including the uncertainty of Stark corrections, are given in parentheses.

n	$d_{3/2}$-$f_{5/2}$	$d_{5/2}$-$f_{7/2}$	$d_{3/2}$-$g_{7/2}$	$d_{5/2}$-$g_{9/2}$	$d_{3/2}$-$h_{9/2}$	$d_{5/2}$-$h_{11/2}$
22	8167.05 (0.50)	8177.69 (0.50)	8899.83 (0.59)	8909.59 (0.59)		
23	7150.62 (0.51)	7159.71 (0.51)	7791.87 (0.65)	7800.37 (0.65)	7939.91 (1.79)	7948.66 (1.79)
24	6295.79 (0.51)	6303.88 (0.51)	6860.89 (0.75)	6868.36 (0.75)		
25	5571.92 (0.52)	5579.10 (0.52)	6071.33 (0.90)	6078.01 (0.90)	6187.82 (2.66)	6195.07 (2.66)
26	4954.66 (0.53)	4960.89 (0.53)	5399.57 (1.11)	5405.47 (1.11)	5501.83 (3.34)	5509.98 (3.34)
27	4425.61 (0.55)	4430.99 (0.55)	[4821.23]	4826.63 (1.38)	4914.06 (4.24)	4919.31 (4.24)
28	3968.87 (0.58)	3973.87 (0.58)	[4325.36]	4330.21 (1.74)	[4407.59]	4412.34 (5.38)
29	3571.94 (0.63)	3576.81 (0.63)				
30	3228.23 (0.70)	3231.93 (0.70)				

gularities adjacent to the nominally clean and flat conducting surfaces partially coated with condensed Na.

All spectra reported here exhibited well-defined SFI signatures. Attempts to measure higher l state transitions (e.g., d-i or d-k) were unsuccessful not only because these higher-order processes required more rf power than was available but also because where a possible SFI signature was obtained it was found to vary as a function of oscillator frequency, indicating that a mixture of states rather than a unique l state was being excited. This change of character places a maximum-n limitation on lower-l measurements as well. For n above about 31 the residual electric field is sufficient not only to cause unacceptable shifts in the transition frequency but also for sufficiently high microwave powers to produce a broadening of the SFI signature indicating a mixing of the $l=3$, 4, and 5 levels. Until better definition of the electric field is possible $n=30$ represents the limit for good resolution of d-f transitions while $n=28$ is the maximum for measurement of d-g and d-h transitions in this apparatus.

IV. REVIEW OF PRIOR DATA

Microwave transitions between d, f, g, and h Rydberg levels of Na were reported more than a decade ago by Gallagher and co-workers. Single-photon transitions $nd_{3/2}$-$nf_{5/2}$ and $nd_{5/2}$-$nf_{7/2}$ were reported[6] for $n=11-17$ with error bars 0.2–1.2 MHz together with the weaker $nd_{5/2}$-$nf_{5/2}$ for $n=11-16$. Two-photon transitions[7] were reported for $nd_{3/2}$-$ng_{7/2}$ and $nd_{5/2}$-$ng_{9/2}$ intervals, $n=13-17$, with error bars from 0.6 to 1.8 MHz. The three-photon nd-nh transitions were reported for $j=\frac{3}{2}$-$\frac{9}{2}$ ($n=13-15$) and $j=\frac{5}{2}$-$\frac{11}{2}$ ($n=13-16$) with error bars 3–4 MHz (except 15 MHz for $n=16$). Rf Stark shifts were extrapolated to zero.

In more recent work[14] the nd-nf transitions for $n=9-12$ were measured with a tenfold improvement in accuracy compared to the previous work. It was established that the f-state fine-structure splitting $nf_{5/2}$-$nf_{7/2}$ was about 5% smaller than the hydrogenic value $\alpha^2/2n^3l(l+1)$ a.u. for $n\geq 9$.[13,14] The ng and nh fine-structure splittings are consistent with hydrogenic values.[6,7]

Although other precise work has been reported on d-state fine structure[21–24] and $\Delta n=1$ transitions in Na,[25] the above constitutes the complete body of accurate nd-nf-ng-nh spectroscopic information in Na Rydberg states to the present.

V. SERIES FITTING FORMULAS, nl-nl'

A. Introduction to series formulas

Series formulas have been of considerable utility for data analysis in s-state-core Rydberg atoms.[26–29] It has been shown empirically[26–28] that level separations nl-nl' can be fitted by smooth inverse-power formulas of the type

$$\nu(n)=\sum_{M=3} A^{(M)}/n^M . \quad (1)$$

The coefficient $A^{(3)}$ of the leading, or $1/n^3$, term is proportional to the difference of the n-independent parts of the quantum defects of the initial and final states.[26] The remaining coefficients can be related to further terms in Rydberg-Ritz series expansions of the quantum defects. It has been possible to fit a wide variety of experimental data satisfactorily with only two or three terms.[28] Series fits serve to identify individual data points of questionable reliability and to predict resonance frequencies for transitions not previously measured. For sufficiently high n it is possible, based on lower-n data, to predict resonance frequencies more accurately than they can be measured directly.

Prior work has shown that for a data set that extends over many n values the most successful three-parameter fits are obtained with (3,5,7) or (3,4,5) models and that these are considerably better than the best two parameter model, the (3,5). [We identify the model by listing the exponents M that are included in the summation (1).] There is some evidence[26] that data sets that include a few low-n values are better fitted by (3,5,7), but a long series that includes several higher-n values may be better fitted by (3,4,5).

B. Series analyses of the present data

Each of the six resonance series indicated in Table I were fitted by formulas of type (1), including data from Refs. 6, 7, 14, and the present work. Each datum was weighted as $1/\sigma^2$ (where σ is the standard deviation). An examination of residuals demonstrated that the observed resonance frequencies departed increasingly from the smooth fits as n increased beyond 25, falling as much as 1–2 MHz below them. Such a deviation is uncharacteristic of any missing exponent $M > 3$ and is consistent with negative quadratic Stark shifts in a background field F.[30] In order to correct for these Stark shifts[31] a term $C(l,l')n^7F^2$ was added to (1) for $n \geq 22$, and the data were refitted to find F. $C(l,l')n^7$ is an estimate of the average quadratic Stark coefficient for components of the nlj-$nl'j'$ resonance. Values of $C(l,l')$ were calculated from second-order perturbation theory with the results $C(d,f)(28)^7 = -600$, $C(d,g)(28)^7 = -3300$, and $C(d,h)(28)^7 = -10\,400$ [all in units MHz (V/cm)$^{-2}$]. (The observed quadratic Stark shift for $28d$-$28f$ reported in Sec. II is considered to be compatible with this theoretical estimate.) Consistent fitted values of F were obtained among the six resonance series, yielding a weighted aver-

TABLE II. Coefficients of (3,4,5) series formulas for field-free Na d-f, d-g, d-h, and d fine-structure intervals. Data from Tran *et al.* (Ref. 14) for $n = 11$ and 12 d-f transitions replaced earlier, lower-precision values from Gallagher *et al.* (Ref. 6). Otherwise, all available data $n = 9$–30 were included in each $l - l'$ series fit. Marginal SD's are given in parentheses. Conditional SD's are given in square brackets. The last column is the reduced χ square, or $\Sigma_n[(\nu_{\text{expt}} - \nu_{\text{fit}})/\sigma]^2$ divided by the number of degrees of freedom, $N - 3$, where N is the number of n values in the data set, and σ are the SD's from Table I.

Series	n values	Expansion coefficients (GHz) $A^{(3)}$	$A^{(4)}$	$A^{(5)}$	χ^2
$d_{3/2}$-$f_{5/2}$	9–17,22–30	87 340.33 (7.23) [0.07]	2546.57 (147.07) [0.69]	−237 993.89 (739.98) [6.63]	3.1
$d_{5/2}$-$f_{7/2}$	9–17,22–30	87 452.87 (11.52) [0.13]	2521.92 (237.30) [1.36]	−238 292.20 (1217.19) [13.96]	6.9
$d_{3/2}$-$g_{7/2}$	13–17,22–26	95 118.52 (66.03) [2.39]	5360 (2171) [36]	−287 901 (17 507) [525]	2.4
$d_{5/2}$-$g_{9/2}$	13–17,22–28	95 308.87 (84.46) [3.09]	2056 (2777) [47]	−258 185 (22 502) [690]	4.7
$d_{3/2}$-$h_{9/2}$	13–15,23,25–27	96 666.66 (52.69) [2.00]	15123 (1807) [28]	−376 101 (14 987) [395]	0.10
$d_{5/2}$-$h_{11/2}$	13–16,23,25–28	96 911.95 (76.44) [2.84]	10 281 (2627) [40]	−336 496 (21 816) [562]	0.2
$d_{3/2}$-$d_{5/2}$	9–17,21–32,34 35,38,40[a]	102.24 (0.73) [0.05]	−107.50 (17.35) [0.49]	150.27 (103.44) [4.89]	0.3

[a]References 6, 7, and 21–24.

age $\langle F \rangle = 21 \pm 12$ mV/cm. This residual field is also consistent with the upper bound on the z component noted in Sec. II. Each resonance frequency $n = 22-30$ was then corrected by removing the estimated Stark shift in field $\langle F \rangle$, and the standard deviations were enlarged by adding the Stark-shift uncertainties to the random-error SD's in quadrature. The resulting corrected resonance frequencies, given in Table I, represent the present measurements of field-free intervals in Na.

The corrected data and uncertainties, together with earlier results, were fitted again by (1) to extract optimal values of parameters $A^{(M)}$, and the parameter uncertainties were taken as marginal and conditional SD's from the variance-covariance matrix of the parameters.[32] Since the basis functions defined by $1/n^M$, taken over the set of n values represented in the data, are highly nonorthogonal, the parameter errors were strongly correlated. Conditional parameter SD's, which correspond to variation of one parameter while all others retain their best values, were frequently two orders of magnitude smaller than marginal SD's, which correspond to variation of a parameter with correlated variations in the others to minimize the overall fitting error. In every case the lowest reduced χ square (χ^2) was obtained with (3,4,5) models. For the two d-f series χ squares for (3,5,7) and (3,5,6) models were generally about twice as large, and those for (3,5) models were typically a factor 20 larger, than for (3,4,5). For d-g and d-h series the model differences were smaller but significant. Coefficients for (3,4,5) models are given in Table II.

The fits reveal that the measured $15d_{5/2}$-$15f_{7/2}$ frequency is anomalously low, by as much as 4 MHz out of 25 600 MHz. The two $n = 14$ d-g frequencies appear low by as much as 7 MHz out of 34 300 MHz. Others of the $n = 13-17$ frequencies lie several error bars from the fits. Frequencies for $n = 29$ d-f likewise appear to be low by as much as 1.5 MHz out of 3570 MHz. Otherwise the (3,4,5) series formulas fit the data well.

Figure 3 illustrates the typical results of series fits. It can be seen in Fig. 3(a) that the (3,4,5) model successfully fits both low- and high-n data except for the scatter at $n = 13-17$, which is apparently of an experimental origin. No other three-parameter fit is as good as (3,4,5), and the (3,5) model is far worse than any of the three-parameter models. Satisfactory behavior of the (3,4,5) fits does not prove that they represent a fundamental property of the level separations, but it establishes the (3,4,5) as the most useful inverse-power model, having no more than three coefficients, by which to test the internal consistency of each data set. The predicted frequencies based on a (3,4,5) fit constitute a smoothed series that optimally transfers information from all measured n's to a desired n.

VI. REANALYSIS OF CORE POLARIZABILITIES

With the considerably expanded data set it is now appropriate to redetermine the Na^+ core dipole and quadrupole polarizabilities by the method of Freeman and Kleppner.[8] In doing this it is also possible to make use of the latest experimental information on the f-state fine structure[14] and to consider the effect of alternate values

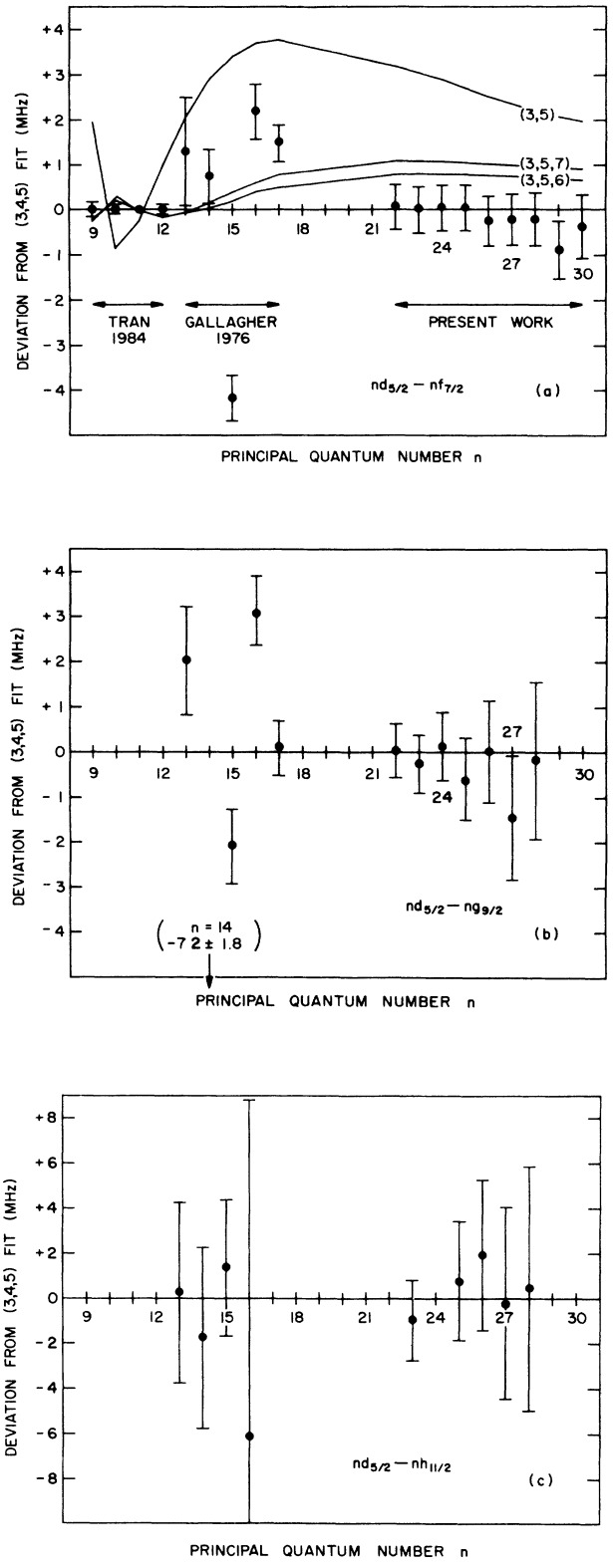

FIG. 3. Deviations of Stark-corrected microwave resonance data from best fits using Eq. (1) with a (3,4,5) model. (a) $nd_{5/2}$-$nf_{7/2}$, including measurements from Refs. 6, 7, and 14. Alternate fits using other exponents are also shown. (b) $nd_{5/2}$-$ng_{9/2}$, including data from Ref. 7 ($n = 13-17$) and present work. (c) $nd_{5/2}$-$nh_{11/2}$, data from Ref. 7 ($n = 13-16$) and present work.

of the penetration energy on the inferred polarizabilities.[10–12]

The core-polarizability analysis requires that the spin-orbit and relativity fine structure and the core penetration be removed so that effective nl-nl' intervals can be used as input data. To remove ambiguity about how this has been done we give the steps explicitly here. In addition to the level shifts arising from core polarization, hydrogenic states $l>0$ are displaced downward in energy from the corresponding Bohr levels by an amount

$$A_n[1/(l+1/2)-3/4n] \text{ a.u.} \tag{2}$$

because of relativistic variation of mass with velocity, where $A_n=\alpha^2/2n^3$ and α is the fine-structure constant.[33] The fine-structure level $j=l+\frac{1}{2}$ is further shifted upward by an amount $lS_l/(2l+1)$, and level $j=l-\frac{1}{2}$ is shifted downward by $(l+1)S_l/(2l+1)$, where S_l is the spin-orbit splitting. In hydrogen,

$$S_l^H=A_n/l(l+1) \text{ a.u.} \tag{3}$$

The fine-structure displacements of the nonhydrogenic $nd_{3/2}$ and $nd_{5/2}$ states are represented simply by $\Delta_{3/2}$ and $\Delta_{5/2}$, respectively. Each level nl is further depressed by core penetration by an amount P_{nl}. Thus the resonance frequencies can be represented by the following expressions, where E_d, E_f, E_g, and E_h are the energy levels without relativity, spin orbit, and penetration:

$$\nu(nd_{3/2}\text{-}nf_{5/2})=E_f-2A_n/7-4S_f/7-E_d-\Delta_{3/2}-P_{nf}+P_{nd}\ , \tag{4a}$$

$$\nu(nd_{5/2}\text{-}nf_{7/2})=E_f-2A_n/7+3S_f/7-E_d-\Delta_{5/2}-P_{nf}+P_{nd}\ , \tag{4b}$$

$$\nu(nd_{3/2}\text{-}ng_{7/2})=E_g-2A_n/9-5S_g/9-E_d-\Delta_{3/2}-P_{ng}+P_{nd}\ , \tag{4c}$$

$$\nu(nd_{5/2}\text{-}ng_{9/2})=E_g-2A_n/9+4S_g/9-E_d-\Delta_{5/2}-P_{ng}+P_{nd}\ , \tag{4d}$$

$$\nu(nd_{3/2}\text{-}nh_{9/2})=E_h-2A_n/11-6S_h/11-E_d-\Delta_{3/2}-P_{nh}+P_{nd}\ , \tag{4e}$$

$$\nu(nd_{5/2}\text{-}nh_{11/2})=E_h-2A_n/11+5S_h/11-E_d-\Delta_{5/2}-P_{nh}+P_{nd}\ . \tag{4f}$$

Equations (4a)–(4f) may be combined so that the d-state variables drop out, and we have

$$E_g-E_f=[\nu(nd_{3/2}-ng_{7/2})+\nu(nd_{5/2}-ng_{9/2})-\nu(nd_{3/2}-nf_{5/2})-\nu(nd_{5/2}-nf_{7/2})]/2-\tfrac{4}{63}A_n+\tfrac{1}{18}S_g-\tfrac{1}{14}S_f+P_{ng}-P_{nf}\ , \tag{5a}$$

$$E_h-E_g=[\nu(nd_{3/2}-nh_{9/2})+\nu(nd_{5/2}-nh_{11/2})-\nu(nd_{3/2}-ng_{7/2})-\nu(nd_{5/2}-ng_{9/2})]/2-\tfrac{4}{99}A_n+\tfrac{1}{22}S_h-\tfrac{1}{18}S_g+P_{nh}-P_{ng}\ . \tag{5b}$$

We assume in Eqs. (4) and (5) that the l-dependent relativity displacement of both $j=l\pm\frac{1}{2}$ levels retains its hydrogenic value [Eq. (2)] for f, g, and h states, i.e., that it is not affected at the 5% level like the spin-orbit splitting. This is a reasonable assumption since the relativity effect depends on $\langle 1/r\rangle$ and $\langle 1/r^2\rangle$ while spin-orbit depends on $\langle 1/r^3\rangle$.[33]

We have used the d-f-g-h intervals measured in the present work and compiled from Gallagher and coworkers[6,7,14] to find E_g-E_f and E_h-E_g for $n=13$–17 and 22–28 (Table III). [The comparable splittings designated $\Delta E_{\text{expt}}(l,l')$ in Ref. 8 include penetration but not relativity or spin-orbit contributions.] The f-state fine-structure splitting S_f was taken 5% less than hydrogenic. In three cases ($27d$-$27g$, $28d$-$28g$, and $28d$-$28h$) where only one of the two fine-structure transitions was observed, the other was calculated based on fitted d-state intervals (Table II) and hydrogenic g and h intervals. P_{nf} was estimated by using $\langle n^3E_{\text{pen}}\rangle/n^3$ calculated from Table III of Ref. 8, then doubled to account for exchange polarization and distortion according to Patil.[12] The result, retaining the same error bar estimated by Freeman and Kleppner, is $P_{nf}=(1.309\pm0.220)\times10^5/n^3$ MHz. The penetration for $l\geq4$ is negligible at the present level of accuracy.[8,10–12] All uncertainties were combined in quadrature. According to the perturbation-theory model for core polarization,[8,9]

TABLE III. Effective energy separations of angular momentum levels after removal of penetration and fine structure, Eq. (5), and coefficients of the core-polarization model, Eq. (6). Data for $n=13$–17 were derived from Gallagher *et al.*, Refs. 6–14. Data for $n=22$–28 are based on the present work. A least-squares fit of these separations using Eq. (6) yields the polarizabilities Eq. (7) with reduced χ square 0.68, $P(\chi^2)=83\%$. The root-mean-square deviation of the fit is 2.0 MHz.

n	l-l'	Separation (MHz)	A_d (MHz)	A_Q (MHz)
13	f-g	3441.33±10.07	3395.89	146.92
13	g-h	802.78±2.95	807.47	10.11
14	f-g	2756.11±8.10	2725.71	118.53
14	g-h	655.34±3.03	649.11	8.20
15	f-g	2253.07±6.60	2220.54	96.96
15	g-h	534.54±2.34	529.45	6.74
16	f-g	1858.65±5.41	1832.66	80.30
17	f-g	1549.79±4.52	1529.97	67.22
22	f-g	718.96±2.21	708.91	31.41
23	f-g	629.24±1.99	620.74	27.54
23	g-h	147.57±1.90	148.71	1.94
24	f-g	554.48±1.83	546.59	24.27
25	f-g	490.04±1.75	483.79	21.50
25	g-h	116.31±2.81	115.96	1.52
26	f-g	436.63±1.75	430.24	19.13
26	g-h	102.97±3.52	103.15	1.35
27	f-g	388.39±1.86	384.31	17.10
27	g-h	92.38±4.46	92.15	1.21
28	f-g	349.92±2.09	344.69	15.35
28	g-h	81.85±5.65	82.67	1.09

$$E_l - E_{l'} = \alpha'_d A_d(l,l') + \alpha'_Q A_Q(l,l') , \quad (6)$$

where A_d and A_Q are expressions related to hydrogenic expectation values $\langle r^{-k} \rangle$, $k=4$ and 6 (given by Freeman and Kleppner[8]) and α'_d and α'_Q are the effective dipole and quadrupole core polarizabilities, respectively. In Table III, A_d and A_Q in atomic units are multiplied by 1 a.u. of frequency (6.57968×10^9 MHz) so that (6) gives the polarizabilities in a.u. when $E_l - E_{l'}$ is in MHz.

The available data for $E_l - E_{l'}$ were fitted by least squares to find n-independent values of α'_d and α'_Q. The results are

$$\alpha'_d = 0.9980\ (0.0033)\ [0.0009]\ \text{a.u.} ,$$
$$\alpha'_Q = 0.351\ (0.081)\ [0.022]\ \text{a.u.} \quad (7)$$

Marginal SD's are given in parentheses and conditional SD's are given in square brackets. A very strong correlation (product-moment correlation coefficient -0.963) exists between the parameters in the fit, and so errors as large as the marginal uncertainties are probable only if corresponding errors occur in both polarizabilities. The results were somewhat affected by the choice of penetration values P_{nf} and by the f-state fine-structure deficit. The sensitivities to changes in the assumed penetration may be expressed as

$$\Delta\alpha'_d = (+5.3\times10^{-8}\ \text{a.u./MHz}) n^3 \Delta P_{nf} ,$$
$$\Delta\alpha'_Q = (-4.2\times10^{-6}\ \text{a.u./MHz}) n^3 \Delta P_{nf} , \quad (8)$$

for corresponding change ΔP_{nf} in MHz. A return to the full hydrogenic value of f-state spin-orbit splitting changes the inferred polarizabilities by a negligible $\Delta\alpha'_d = +3\times10^{-6}$ a.u. and $\Delta\alpha'_Q = -3\times10^{-4}$ a.u. Freeman and Kleppner reported $\alpha'_d = 1.0015\pm0.0015$ a.u. and $\alpha'_Q = 0.48\pm0.15$ a.u.

Eissa and Öpik[34] have analyzed the nonadiabatic effects in the adjustment of the polarized core wave function to motion of the valence electron. With the Eissa and Öpik correction based on Na($4f$) applied to the present results, static core polarizabilities are

$$\alpha_d = 0.9941, \quad \alpha_Q = 1.690 . \quad (9)$$

Other experimental and theoretical values of the polarizabilities are given in the references.[11,12,35] The nonadiabatic corrections are expected to depend slowly on n.

TABLE IV. Coefficients of (3,4,5) series formulas for Na level separations, $5 \le l \le 9$. The coefficients for transitions between the upper fine-structure levels are given explicitly. Coefficients for transitions between the lower fine-structure levels may be obtained by adding $350\,400/l(l+1)(l+2)$ MHz to $A^{(3)}$.

Series	$l \to l+1$	Expansion coefficients (MHz) $A^{(3)}$	$A^{(4)}$	$A^{(5)}$
$h_{11/2}$-$i_{13/2}$	5-6	588 399	+ 884	−4 112 000
$i_{13/2}$-$k_{15/2}$	6-7	228 477	−1191	−2 158 000
$k_{15/2}$-$l_{17/2}$	7-8	101 922	−3826	−1 229 000
$l_{17/2}$-$m_{19/2}$	8-9	50 440	−2065	−761 300

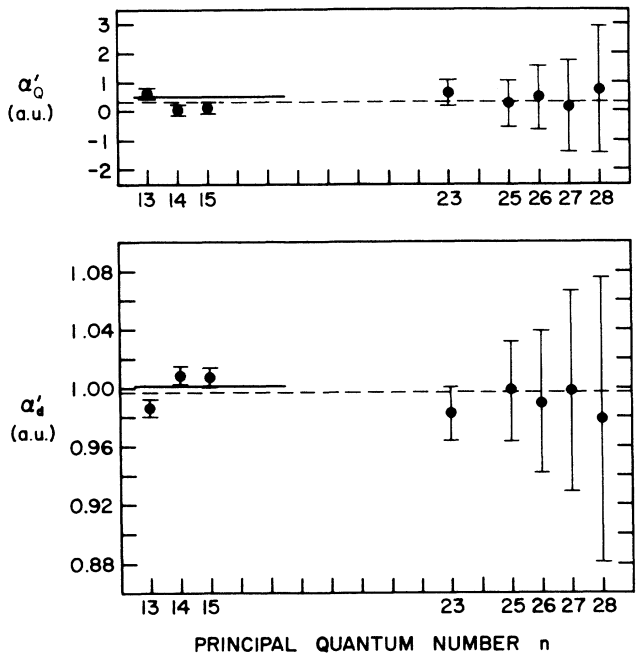

FIG. 4. Effective dipole (α'_d) and quadrupole (α'_Q) core polarizabilities for individual n values, $n=13$–28. The dashed lines indicate the all-n results Eq. (7), and the solid lines are the results of the analysis by Freeman and Kleppner, Ref. 8.

For each n for which experimental values of both E_g-E_f and E_h-E_g are available, the pair of equations (6) can be inverted to yield the core polarizabilities directly. Figure 4 shows the individual values for $n=13$–15, 23, and 25–28. No trend with increasing n is discernible at the present level of accuracy.

For convenience in future work Table IV lists (3,4,5) expansion coefficients [see Eq. (1)] for level separations $l \to l+1$ for $l \ge 5$, $j = l+\frac{1}{2} \to l+\frac{3}{2}$. The coefficients are based on the polarizabilities (7) and hydrogenic fine structure and represent within ±5 kHz the predictions of the core-polarization model between $n=10$ and 30. These may be used directly or may be combined with lower-l intervals (e.g., Table II) to give expected frequencies for multiphoton transitions, exclusive of rf or dc Stark shifts, within about 1 MHz. Level separations for $j = l-\frac{1}{2} \to l+\frac{1}{2}$ may be obtained from Table IV by adding $\alpha^2/l(l+1)(l+2)$ a.u. to the coefficient $A^{(3)}$.

VII. CONCLUSIONS

New microwave resonance frequencies have been reported for *nd-nf*, *nd-ng*, and *nd-nh* transitions in Na $n=22$–30. From these, together with older data, six Rydberg series of level separations can be modeled accurately (to about 1 MHz) by corresponding three-term formulas. Statistical or systematic errors in earlier data that are much larger than originally estimated have been highlighted. Since it was the data at $n=13$–17 that was formerly used for the analysis of core polarizabilities in Na, a considerable improvement in reliability may be expected by inclusion of the new data. Values of the

effective dipole and quadrupole polarizabilities α'_d and α'_Q have now been inferred from data spanning $n=13-28$. The new and old values have overlapping error bars, which reflects both the compatibility of the two data sets and the much larger statistical weight of the earlier set. The effective dipole polarizability has an uncertainty comparable to the previous study, while the uncertainty of the quadrupole polarizability has been reduced about fourfold (taking the geometric mean of marginal and conditional uncertainties). Measurements of higher accuracy for f, g, and h intervals, $n=10-30$, and especially measurement of intervals with $l>5$, would be required to reveal the n dependence, if any, of both polarizabilities.

The present measurements fulfill the original objective of establishing the high-n, $2\leq l\leq 5$ spectroscopy of Na with high accuracy and allowing an assessment of stray electric fields. It was possible to do both things at once because of the very different, and well-understood, n dependences of core and Stark interactions. Work remains to be done to understand more fully the selective field ionization of the $l\geq 3$ levels, in particular how the Na diabatic SFI spectra relate to calculated hydrogenic SFI spectra, and how they depend on ambient fields and on the rate of increase of the ionizing electric field.

ACKNOWLEDGMENT

This work was supported by the National Science Foundation under Grant No. PHY-8507532.

[1]K. B. MacAdam, R. G. Rolfes, and D. A. Crosby, Phys. Rev. A **24**, 1286 (1981).
[2]K. B. MacAdam, D. B. Smith, and R. G. Rolfes, J. Phys. B **18**, 441 (1985).
[3]K. B. MacAdam, R. G. Rolfes, X. Sun, and D. B. Smith, Nucl. Instrum. Methods B **24/25**, 280 (1987).
[4]K. B. MacAdam, R. G. Rolfes, X. Sun, J. Singh, W. L. Fuqua III, and D. B. Smith, Phys. Rev. A **36**, 4254 (1987).
[5]I. L. Beigman and M. I. Syrkin (unpublished).
[6]T. F. Gallagher, R. M. Hill, and S. A. Edelstein, Phys. Rev. A **13**, 1448 (1976).
[7]T. F. Gallagher, R. M. Hill, and S. A. Edelstein, Phys. Rev. A **14**, 744 (1976).
[8]R. R. Freeman and D. Kleppner, Phys. Rev. A **14**, 1614 (1976).
[9]B. Edlen, *Spectroscopy I*, Vol. XXVII of *Handbuch der Physik* (Springer, Berlin, 1964), p. 80; also see J. E. Mayer and M. G. Mayer, Phys. Rev. **43**, 605 (1933).
[10]C. E. Theodosiou, Phys. Rev. A **28**, 3098 (1983).
[11]J. C. Lombardi, Phys. Rev. A **32**, 2569 (1985).
[12]S. H. Patil, Phys. Rev. A **33**, 90 (1986).
[13]T. F. Gallagher, W. E. Cooke, and S. A. Edelstein, Phys. Rev. A **16**, 273 (1977).
[14]N. H. Tran, H. B. van Linden van den Heuvell, R. Kachru, and T. F. Gallagher, Phys. Rev. A **30**, 2097 (1984).
[15]D. A. Crosby and K. B. MacAdam, Rev. Sci. Instrum. **52**, 297 (1980).
[16]T. F. Gallagher, L. M. Humphrey, W. E. Cooke, R. M. Hill, and S. A. Edelstein, Phys. Rev. A **16**, 1098 (1977).
[17]T. H. Jeys, G. W. Foltz, K. A. Smith, E. J. Beiting, F. G. Kellert, F. B. Dunning, and R. F. Stebbings, Phys. Rev. Lett. **44**, 390 (1980).
[18]J. Singh, X. Sun, and K. B. MacAdam, Phys. Rev. Lett. **58**, 2201 (1987).
[19]N. L. S. Martin and K. B. MacAdam, J. Phys. B **19**, 2435 (1986).
[20]C. E. Theodosiou, Phys. Rev. A **30**, 2881 (1984).
[21]T. H. Jeys, K. A. Smith, F. B. Dunning, and R. F. Stebbings, Phys. Rev. A **23**, 3065 (1981).
[22]G. Leuchs and H. Walther, Z. Phys. A **293**, 93 (1979).
[23]C. Fabre, M. Gross, and S. Haroche, Opt. Commun. **13**, 393 (1975).
[24]T. F. Gallagher, L. M. Humphrey, R. M. Hill, W. E. Cooke, and S. A. Edelstein, Phys. Rev. A **15**, 1937 (1977).
[25]C. Fabre, S. Haroche, and P. Goy, Phys. Rev. A **18**, 229 (1978); **22**, 778 (1980).
[26]K. B. MacAdam and W. H. Wing, Phys. Rev. A **13**, 2163 (1976).
[27]W. H. Wing and K. B. MacAdam, in *Progress in Atomic Spectroscopy, Part A*, edited by W. Hanle and H. Kleinpoppen (Plenum, New York, 1978), p. 491.
[28]J. W. Farley, K. B. MacAdam, and W. H. Wing, Phys. Rev. A **20**, 1754 (1979).
[29]T. N. Chang, J. Phys. B **7**, L108 (1974).
[30]C. Fabre and S. Haroche, Opt. Commun. **15**, 254 (1975); A. F. J. van Raan, G. Baum, and W. Raith, J. Phys. B **9**, L349 (1976); T. H. Jeys, M. C. Copel, G. B. McMillian, F. B. Dunning, and R. F. Stebbings, *ibid.* **16**, 3747 (1983).
[31]A similar procedure was used in Ref. 26 to correct Rydberg intervals in He ($n=16-18$) for Stark shifts in a small residual field.
[32]W. C. Hamilton, *Statistics in Physical Science* (Ronald, New York, 1964).
[33]H. Bethe and E. E. Salpeter, *Quantum Mechanics of One and Two Electron Atoms* (Springer, Berlin, 1957).
[34]H. Eissa and U. Öpik, Proc. Phys. Soc., London **92**, 556 (1967).
[35]S. Krishnagopal, S. Narasimhan, and S. H. Patil, J. Chem. Phys. **83**, 5772 (1985).